JCBPS; Section A; May 2017 – July, 2017, Vol. 7, No. 3; 547-562. E- ISSN: 2249 –1929

[DOI: https: //doi.org/10.24214/jcbps.A.7.3.54762]

Journal of Chemical, Biological and Physical Sciences

An International Peer Review E-3 Journal of Sciences

*Available online at*www.jcbsc.org

Section A: Chemical Sciences

CODEN (USA): JCBPAT Research Article

Potential Biological Activities, Molecular Docking and Synthesis of Novel Ag^{+}, Ni $^{+2}$ and Fe^{+3} Complexes with Schiff base *N'*-(1-(4-((3,4-dihydroquinolin-1(2*H*)-yl)sulfonyl) phenyl)ethylidene)-3-oxo-3*H*-benzo[*f*]chromene-2-carbohydrazide

Mahmoud Sayed Bashandy[1,2], Sami Abdullah Al-Harbi[1], Amr M. Nassar[2,3], Shimaa Mohamed Abd El-Gilil[4]

[1]Department of Chemistry, University College in Al-Jamoum, Umm Al-Qura University, 21955, Makkah, Saudi Arabia

[2]Department of Chemistry, Faculty of Science (Boys), Al-Azhar University, Nasr City, 11884, Cairo, Egypt

[3]Department of Chemistry, College of Science, Aljouf University, Sakaka, Saudi Arabia

[4]Department of Pharmaceutical Organic Chemistry, Faculty of Pharmacy (Girls), Al-Azhar University, Nasr City, 11754, Cairo, Egypt

Received: 21 May 2017**; Revised:** 31 May 2017; **Accepted:** 7 June 2017

Abstract: Ag^{+}, Ni^{+2} and Fe^{+3} complexes with Schiff base *N'*-(1-(4-((3,4-dihydroquinolin-1(2*H*)-yl)sulfonyl)phenyl)ethylidene)-3-oxo-3*H*-benzo-[*f*]chromene-2-carbohydrazide (**HL**) have been synthesized. The structure of the new complexes is established using spectroscopic, elemental and thermal analysis. The data reveals that the geometry of the complexes are dihedral for Silver complex, square planar for Nickel complex and octahedral for Iron complex. The ligand molecule is found to be acts as bidentate with complex **1** through carbonyl oxygen and enol form oxygen and tridentate with complexes **2** and **3** *via* carbonyl oxygen, enol form oxygen and azomethine nitrogen. The structures of the newly synthesized compounds were confirmed by elemental analysis, IR, UV, TGA and Ms spectral data. The *in vitro* antimicrobial activities of ligand and

their complexes were tested. Ni (II) complex showed a significant activity against all microorganisms. Fe (III) complex exhibits a significant activity against Mycobacterium tuberculosis. In addition, *in vitro* cytotoxic activities of all the synthesized compounds were evaluated on human liver carcinoma HEPG2 and human prostate carcinoma PC3 cell lines. **HL**, ligand exhibited a significant inhibition against HEPG2 with IC_{50} value 178.21 µM. while, Ag(I) and Ni(II) complexes exhibited a significant inhibition against PC3 cell line with IC_{50} values 4.39 µM., and 10.68 µM., respectively compared to MTX as a reference drug. Docking studies involving MOE (Molecular Operating Environment) was studied to find the potential binding affinities between the ligand and the DHFR enzyme. **HL** and Ni (II) complex showed more interaction with DHFR which lead to inhibit this enzyme.

Keywords: Sulfonamide, Benzo[*f*]chromene, Anticancer, Molecular docking, Binuclear complexes, Antimicrobial activity

1. INTRODUCTION

The biological activates of Schiff bases and their metal complexes have been played an important role in bioorganic and bioinorganic chemistry. These compounds usually used for a several medicinal applications such as anti [-microbial, -viral, -tumor, -inflammatory, -proliferative, -malarial] and antipyretic compounds[1-7]. It was concluded that, the biological activities of Schiff bases is increased by complexation[8-11]. Tetrahydroquinoline derivatives have widely pharmaceuticals applications[12-17]. The reactions of tetrahydroquinoline with different derivatives, which lead to modification of its medicinal purpose[18-20]. Sulfonamides are known to have a widely applications in several biological systems[21-25]. Many works studied the effect of the presence of sulfonamides, azomethine, tetrahydroquinoline and their metal complexes for increasing the biological activity[25-27].

From this point of view, the present study was undertaken to throw more light on the synthesis and characterization of new Ag^{+}, Ni^{+2} and Fe^{+3} complexes with Schiff base *N'*-(1-(4-((3,4-dihydroquinolin-1(2*H*)-yl)sulfonyl)phenyl)ethylidene)-3-oxo-3*H*-benzo-[*f*]chromene-2-carbohydrazide. The Schiff base, H_2L, ligand and its metal complexes were investigated for antibacterial and antifungal properties. Ten pathogenic microorganisms were used for this investigation. The Gram- positive bacteria used were *Staphylococcus aureus* (RCMB 010027), *Streptococcus pneumoniae* (RCMB 010010) and *Bacillus subtilis* (RCMB 010067). The Gram- negative bacteria were *Pseudomonas aeruginosa* (RCMB 010043-6), *Salmonella Typhimurium* (RCMB 010315-4), *Klebsiella pneumoniae* (RCMB 010096-5) and *Escherichia coli* (RCMB 010052-3). Two fungi, *Aspergillus fumigatus* (RCMB 02568) and *Candida albicans* (RCMB 05036). In addition, Mycobacterium tuberculosis (RCMB 010094-8) was also utilized. Moreover, the newly synthesized compounds were evaluated for their *in-vitro* cytotoxicity against human liver carcinoma HEPG2 and human prostate carcinoma PC3 cell lines.

2. EXPERIMENTAL

2.1. Materials:

2-Cyano-*N'*-(1-(4-((3,4-dihydroquinolin-1(2*H*)-yl)sulfonic)phenyl)ethylidene)acetohydrazide (**QSA**) and 2-hydroxy-1-naphthaldehyde were obtained in line with the approaches stated in the literature[28]. Silver (I), Nickel (II), and Iron (III) ions were used as nitrate salts and organic solvents, source of these materials from Merck, BDH and Sigma-Aldrich

2.2. Instruments

The compounds used were all within the theoretical values of ±0.4%. The FT-IR spectra (4000-400 cm^{-1}) were recorded as KBr disks through the application of FT-IR (Shimadzu) spectrophotometer model 8400. The automated continuums of the ligand and its metallic compounds were prepared in 10^{-3} M DMF solution using an Angstrom UV spectrophotometer approach 1100 under the scope of 200-900 nm. Samples were directly applied to the examination and the disintegrations were done at 300 ºC and 70 *eV*. The Gouy method was applied in the measurement of the magnetic predispositions of the complexities at a room temperature through the application of a magnetic susceptibility balance (Johnson Matthey, Alfa product, Model No. MKI).The effective magnetic moments were computed using the formulae μeff = 2.828 (χM.T) 1/2 B.M., where χM represents the molar predisposition that is corrected through the application of Pascal's coefficients for the diamagnetism of all molecules in the complexes while T; the absolute temperature. The pH and conductometer apparatus Model 14831 (Italy) were applied in the establishment of the molar conductance of the mixtures in moles of the solid compounds in DMF. Similarly, the melting point instrument was applied in the measurement of samples and that were not corrected. TGA data was established from temperature 25~800°C at a warming frequency of 20°C/min in a vigorous N_2 atmosphere. Lastly, The Shimadzu TGA tool was suitable to obtain the data, while the thermal analyzer was equipped with a thermo-balance.

2.3. Synthesis of ligand

To a mixture of compound 2-cyano-*N'*-(1-(4-((3,4-dihydroquinolin-1(2*H*)-yl)sulfonyl)phenyl) ethylidene)acetohydrazide **(QSA)** (3.96 g, 0.01 mol) and 2-hydroxy-1-naphthaldehyde (1.72 g, 0.01 mol) in EtOH (50 mL), a few drops of piperidine was added as catalyst. The reaction mixture was refluxed for 5 h. The isolated product was collected and recrystallized from AcOH to give **HL**. Yellow solids, Yield, 87.3%; mp 270-271 ºC. IR (KBr, cm^{-1}): ν_{max}3176 (NH), 3011 (CH aromatic), 2894 (CH aliphatic), 1700, 1655 (2C=O), 1579 (C=N), 1552 (C=C), 1350, 1166 (SO_2), 1243, 1039 (C-O-C).MS *m/z* (%):553.48 [M^++2](0.50), 552.35[M^++1] (1.16), 551.32 [M^+] (0.21),536.86 (1.65),532.12 (1.08), 507.05 (1.11), 496.01 (2.73), 478.36 (0.68), 322.19 (11.04), 315.10 (33.82), 299.29 (51.56), 295.25 (18.66), 279.17 (14.01), 259.17 (11.66), 258.21 (12.25), 256.27 (30.15), 254.22 (16.01), 250.21 (12.12), 242.24 (14.51), 230.18 (14.81), 212.19 (20.84), 208.19 (17.85), 202.10 (11.47), 197.19 (15.74), 187.15 (23.04), 186.14 (64.47), 181.17 (22.19), 179.17 (25.24), 173.11 (18.61), 167.11 (30.00), 154.15 (26.97), 152.17 (29.66), 144.12 (14.39), 139.16 (49.16), 137.15 (37.66), 134.07 (39.45), 125.16 (26.86), 124.16 (42.61), 122.14 (18.96), 116.09 (26. 87.07 (27.15),03), 114.10 (18.20), 113.12 (19.74), 96.12 (100.00), 94.11 (10.32), 88.08 (12.41), 74.07 (20.61), 72.11 (16.98), 71.11 (63.30), 70.13 (16.78), 56.11 (57.94), 44.05 (53.05), 42.10 (45.62). Anal. Calc. for $C_{31}H_{25}N_3O_5S$ (551.61): C, 67.50; H, 4.57; N, 7.62; S, 5.81. Found: C, 67.33; H, 4.27; N, 7.47; S, 5.59%.

2.4. Synthesis of Complexes

The metal complexes are synthesized by the reaction of Silver, Iron and Nickel nitrates with ligand in 2:1 molar ratio, respectively in refluxing ethanol for 2h. The precipitate formed is filtered, washed several times with hot water and ethanol then dried, **Table 6**.

2.5. Antimicrobial studies

The antibacterial and antifungal activities were evaluated by standardized disc-agar diffusion method[29-31]. The efficacy of the novel compounds was determined against different strains of gram-positive and gram-negative bacteria, also evaluated against different fungal strains. The gram-positive organisms that were

used for culture sensitivity include Staphylococcus aureus (RCMB 010027), Streptococcus pneumoniae (RCMB 010010) and Bacillis subtilis (RCMB 010067). On the other hand, the gram-negative organisms that were used for culture sensitivity include Pseudomonas aeruginosa (RCMB 010043), Salmonella typhimurium (RCMB 010315), Klebsiella pneumoniae (RCMB 0010096) and Escherichia coli (RCMB 010052) and. The fungal strains that were used include Aspergillus fumigatus (RCMB 02568) and Candida albicans (RCMB 05036). Different antibiotics were used as reference for evaluating the antimicrobial activity of novel compounds. Ampicillin, Ciprofloxacin and Amphotericin B were used as the reference antibiotic for assessing the antimicrobial activity of the novel compounds against gram-positive bacteria, gram-negative bacteria and fungal strains respectively.

2.6. Anti-mycobacterial tuberculosis Activity

Mycobacterium tuberculosis (RCMB 010094-8) was used as the experimental microbe for the present study. Isoniazid was used as the reference antibiotic in comparison to the novel compounds. MABA (Microbial Alamar Blue Assay) was conducted to evaluate the antibacterial activity of the novel compounds. The assay was conducted in micro-titer plates. The micro-titer plates were round-bottomed and black in color. Such arrangements were used to prevent the background effects of light. The peripheral wells in the micro-titer plate were filed with sterile water. Sterile water was use to prevent dehydration in the wells. The wells were classified into two types; experimental and control. The experimental wells were filled with novel compounds. However, the control wells consisted of bacterial colony only. The experimental wells were filled with different dilutions of the bacterial colony. Initial dilutions of the novel compounds were achieved with dimethyl sulfoxide. Subsequent dilutions were undertaken in the micro-titer plate. A two-fold dilution was achieved in the micro-titer plate. The experimental and control wells were inoculated with 0.1 ml (10^5 CFU/ml) Mycobacterium tuberculosis. The micro-titer plate was incubated at 37 °C. On the 4^{th} day of experimentation, 20 micro liter of Alamar Blue Solution and 12.5 micro liters of 20 % Tween-80 were added to the micro-titer plate. The micro-titer plate was further incubated for 24 hours at 37 °C. Spectrophotometric readings were recorded at 590 nm. The results were expressed as Percentage inhibition (% inhibition). Percentage inhibition was estimated as:

% inhibition=1-(Mean O.D. of test well/mean O.D. of B wells) × 100.

Results were also expressed as Visual Minimum Inhibitory Concentrations (VMIC). VMIC is defined as the lowest concentration of the novel antimicrobial compounds that prevented color change.

2.7. Anti-tumor activity

The synthesized compounds (dissolved in DMF) were assessed for cytotoxic activity against HEPG2, and PC3 cell lines. The evaluation for the experimental and control cells focused on the ratio for inhibition of cell growth (IC_{50}) by applying the formula[32-35]: (C-T/C) x 100 = IC_{50}.

2.8. Docking and molecular modeling

Dihydrofolate reductase and thymidylate synthase are amongst major goals within antimicrobial and anticancer activity[36,37]. Molecular modeling research by means of Molecular Operating Environment (MOE)[38] unit was conducted to downsize the anticancer action of the lately synthesized compounds. Researches on molecular docking further assist in comprehending the action mode of the composites through their different relations with the dihydrofolate reductase active sites.

3. RESULTS AND DISCUSSION

3.1. IR Spectra

The infrared spectrum of the ligand (**HL**) shows strong bands at1686, 1642and 1602 and 3268 cm^{-1}which are assignable to υ C=O, υ C=N (enol form), υ C=N (Schiff base) and υ O-H. These bands indicates the presence of tautomeric structure in the ligand molecule[39], **Scheme 1-to 4.**

On the other hand, the infrared spectra of the complexes show shift in some bands according to the mode of chelation in both complex molecule as following:-

1. The appearance of band in the range (1707-1710) cm^{-1} in the spectra of the complexes due to C=O group, the shift of this band to higher wave number is assignable to the participation of carbonyl group in chelation with metal ions[40].
2. The deprotonation of hydroxyl groups and participation with metal ions as $–O^-$ is showed from the absence of the band at 3268 cm^{-1} which due to the υ O-H in the free ligand, confirming this, the observed band at 550 cm^{-1} due to υ Ag-O in complex **1** and strong band in the range 481-486 cm^{-1} which assignable to bridging oxygen and the binding[41] with metal ions as M-O-M .
3. The bands observed in the range 1536-1550 cm^{-1}, 1290-1304 cm^{-1} and 1093-1096 cm^{-1} for complexes **2** and **3** are due to ν (N═O), ν_{asym} (NO_2) and ν_{sym} (NO_2) which indicating the presence of unidentate nitrate groups[42].
4. The broadband observes in complexes **2** and **3** in the region 3400-3450 cm^{-1} in complexes **2** and **3** is attributed to the coordinated water molecules[43].

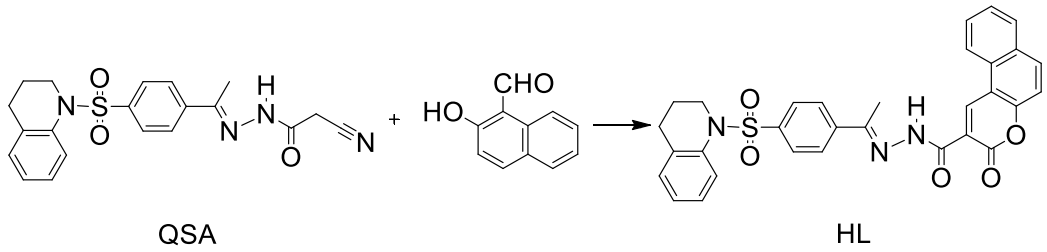

Scheme 1: Schematic equation to preparation of ligand **(HL)**

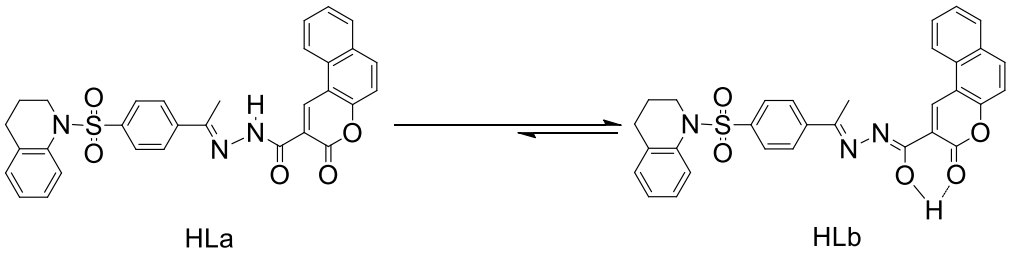

Scheme 2: Schematic equation to tautomerization of ligand (**HL)** from keto form **(HLa)** to enol form **(HLb)**

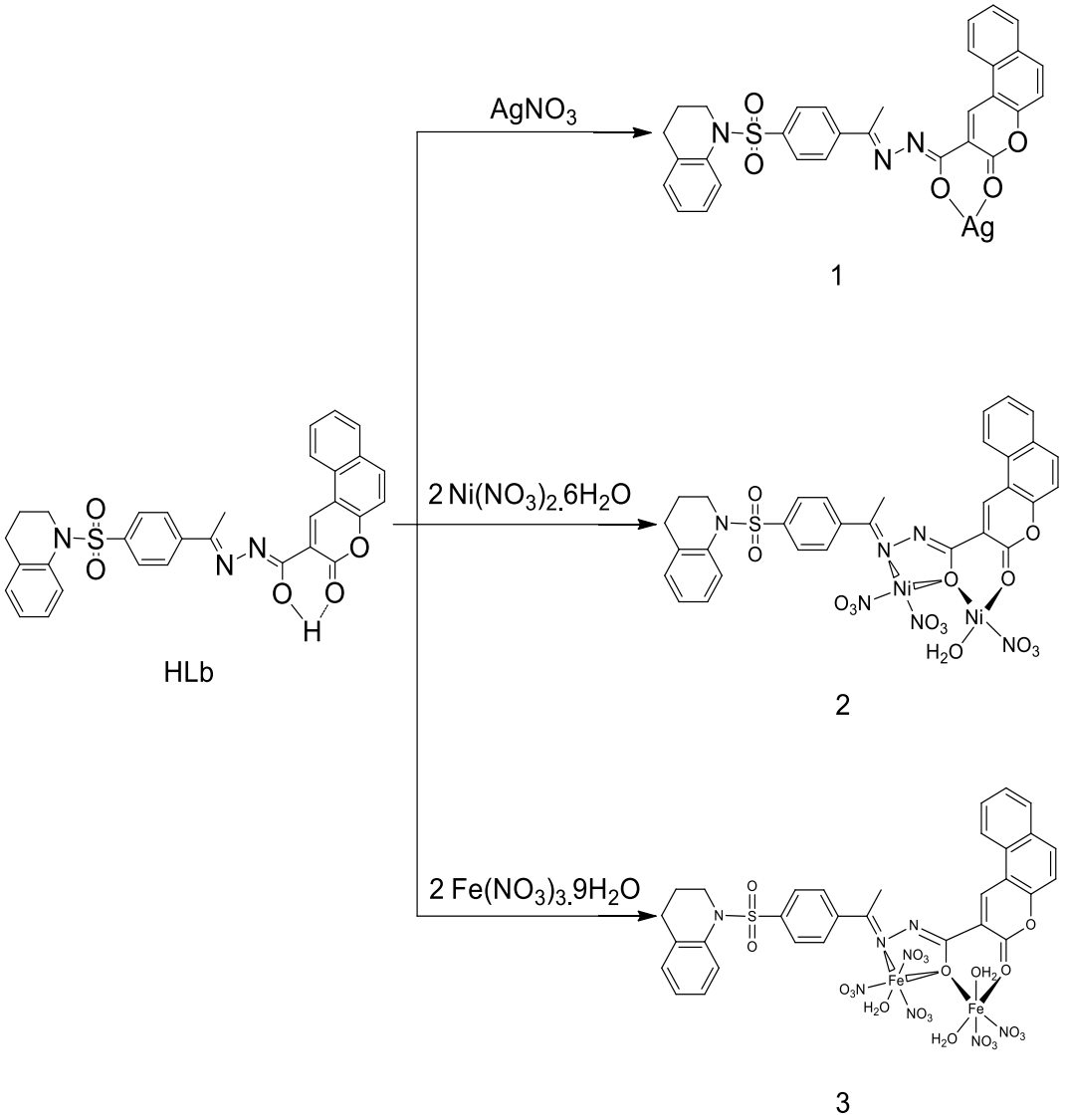

Scheme 3: Schematic equation to preparation of complexes (**1-3**) from ligand (**HL**)

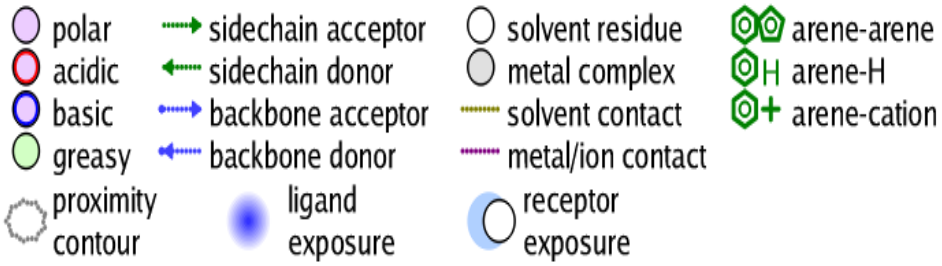

Scheme 4. Representative keys for the type of interactions between the substrates and DHFR

3.2. Electronic Spectrum

The electronic spectrum of the ligand shows two bands at 290and 380 nm in DMF, which may be assigned to the π– π* transition of the phenyl rings and n– π* transitions of the heteroatom moieties respectively. All the complexes show bands in the range 290-295nm, which may be attributed to the π–π* transitions of the phenyl rings. The bands in the region 370-376 nm have been assigned to the n–π* transitions of the heteroatoms moieties.

The UV-Vis spectrum of Fe^{+3} complex **2** exhibits band at 468 nm attributed to $T_{2g}(F) \rightarrow {}_5E_g$ transition in octahedral configuration, respectively. The band observed at 420 nm is due to charge transfer[44].

The Nickel complex **3** shows absorption at 480 nm assignable to d-d transition ($^1A_{1g} \rightarrow {}^1A_{2g}$) which supports the square planar geometry around Ni(II) ions. The charge transfer band is observed[45] at 425 nm

3.3. Thermal gravimetric analysis

The thermogravimetric analysis (TGA) curves for the complexes were obtained at a heating rate of 10 °C/min and flowing nitrogen atmosphere over a temperature range of 20-800 °C. The thermal decomposition was studied as a function temperature by TGA. They exhibit several decomposition steps. The decomposition starts with decomposition of ligand organic parts. The remaining residue of 20-23 % consists of the corresponding a mixture of metal sulphide and metal oxide.

3.4. Antimicrobial activity

The metal ion complexes were assessed for antimicrobial activity against three strain Gram positive bacteria *Staphylococcus aureus* [*RCMB 010027*], *Streptococcus pneumonia* [*RCMB 010010*] and *Bacilli's subtitles* [*RCMB 010067]*), four gram negative bacteria *Pseudomonas aeruginosa* [*RCMB 010043*], *Salmonella Typhimurium (RCMB 010315-4), Klebsiella pneumoniae* [*RCMB 010096-5*], *Escherichia coli* [*RCMB 010052-3*] and the fungi *Aspergillus fumigatus* [*RCMB 02568*], *Candida albicans* [*RCMB 05036*]. The result of the antimicrobial assay of the synthesized compounds is given in **Table 1**. Complex **2** showed significant activity against all microorganisms. However, Complex **3** exhibits a good activity against *Streptococcus pneumonia* as a gram positive bacteria and *Klebsiella pneumoniae* as a gram negative bacteria compared to *Ampicillin* and *Ciprofloxacin* as a reference drug, respectively. The complex **3** exhibits a significant activity against Mycobacterium tuberculosis, **Table 2**.

3.5. In vitro anticancer studies

The newly synthesized compounds were evaluated for their *in-vitro* cytotoxicity against human liver carcinoma HEPG2 cell line **Tables 3**, observe that ligand, **HL** having 3-oxo-3*H*-benzo[*f*]chromene-2-carbo-hydrazide moiety with IC_{50} value (178.21 µM.) showed increased activity when compared to methotrexate with IC_{50} value (239.86 µM.). In addition, compounds were evaluated for their *in-vitro* cytotoxicity against human prostate carcinoma PC3 cell line **Tables 4**, observe that complex **1** having silver atom with IC_{50} value (4.39 µM.), and complex **2** having nickel atom with IC_{50} value (10.68 µM.) showed increased activity when compared to methotrexate with IC_{50} value (30.15 µM.).

3.6. Docking of methotrexate, HL and compounds 1-3 into DHFR:

3.6.1. Docking of methotrexate MTX into DHFR:

The active site revealed that hydrogen bond interactions beside hydrophobic interactions were considered responsible for the observed affinity as it acts as a hydrogen bond donor to the backbone Ile 5, Ile 94 residues, and the side chain Asp 27 residue. It also acts as a hydrogen bond accepter to Arg 52 and Arg 57 residues. This beside many hydrophobic interactions with various amino acid residues: ILe 5, Ala 6, Ala7, Asp 27, Leu 28, Phe 31, Lys 32, Ser 49, Ile 50, Arg 52, Leu 54, Arg 57, Ile 94, Tyr100 and Thr 113, as shown in **Figure 1**.

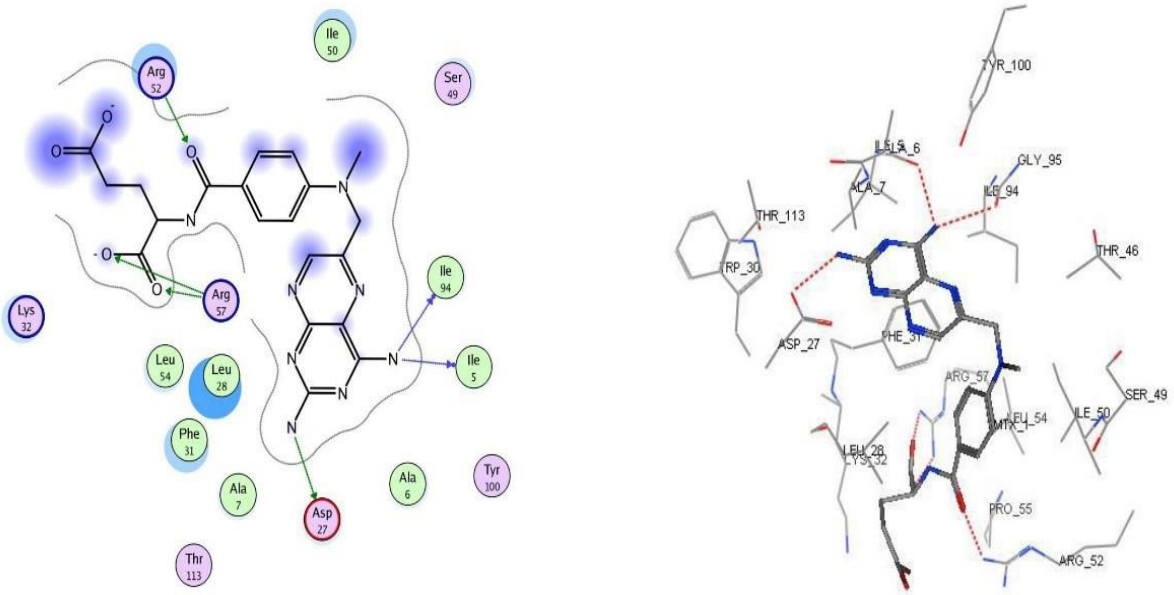

Figure 1: Docking of **MTX** into DHFR

3.6.2. Docking of compound HL into DHFR:

Active site illustrated the presence of two hydrogen bond interactions between one oxygen atom of SO_2 moiety and oxygen atom of carbonyl function as they acted as a hydrogen bond acceptors with the side chain residues Ser 59 and Asn 64 (2.72 Å, 3.38 Å) at a strength of 58.5 % and 6.1 %; respectively, beside many hydrophobic interactions between other atoms of the compound and the following amino acid residues: Ile 16, Gly 20, Asp 21, Leu 22, Arg 28, Phe 31, Phe 34, Gln 35, Thr 56, Ile 60, Pro 61, Asn 64, Val 115, Gly 117 and Tyr 121, as shown in **Figure 2**.

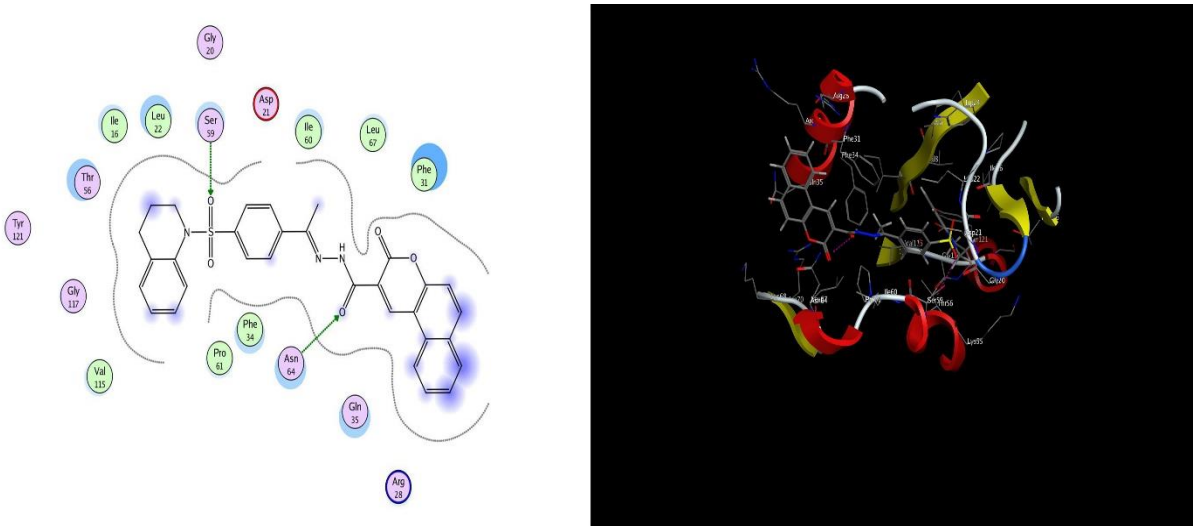

Figure 2: Docking of ligand **HL** into DHFR

3.6.3. Docking of compound 1 into DHFR:

Active site revealed an arene hydrogen interaction between phenyl ring and the side chain residue; Ile 50, in addition to two arene cation interaction between two phenyl rings and the side chain residue; Lys 32. Moreover, it showed an interaction between silver atom and the side chain residue; Leu 28, beside many hydrophobic interactions between other atoms of the compound and the following amino acid residues: Ile 14, Gly 15, Ala 29, Phe 31, Lys 32, Thr 46, Ser 49, Arg 52, Leu 54, Pro 55, Ile 94, Gly 95, Gly 96 and Tyr 100, as shown in **Figure 3**.

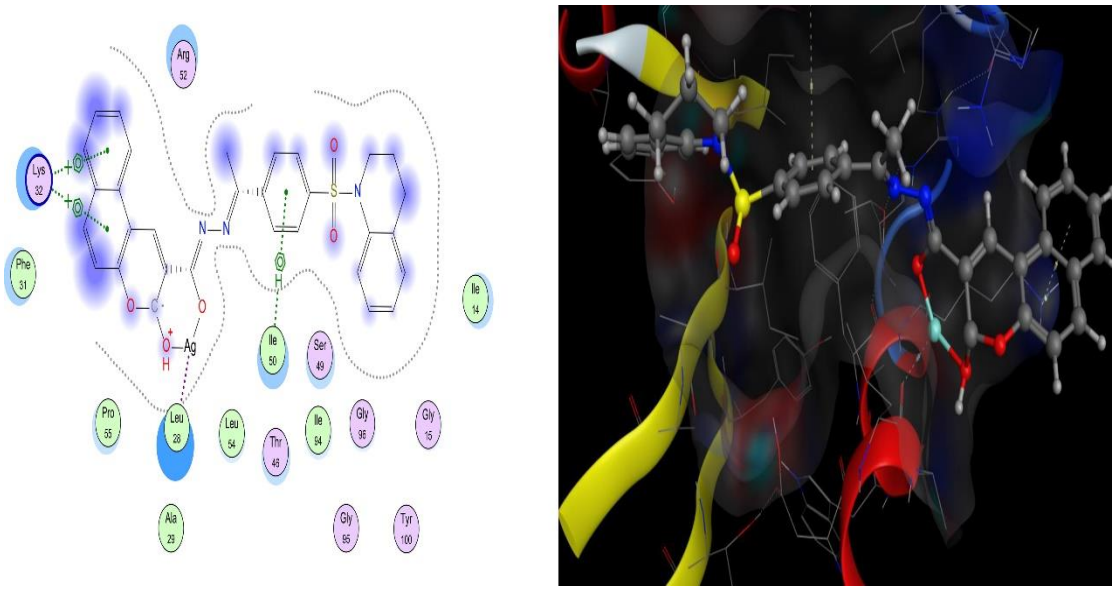

Figure 3: Docking of Complex **1** into DHFR

3.6.4. Docking of compound 2 into DHFR:

Active site illustrated the interactions of the two oxygen atoms of two hydroxyl moieties as it acted as a hydrogen bond donor with the same side chain residue; Ile 14 (2.86 Å, 2.85 Å) at a strength of 7.8 % and 7.3 %; respectively, as well as two oxygen atoms of nitroso functions acted as a hydrogen bond acceptor with the side chain residues; Asp 27 and Tyr 100 (2.99 Å, 3.24 Å) at a strength of 1.4 % and 0.8 %; respectively. Moreover, one oxygen atom of sulfonyl moiety acted as a hydrogen bond acceptor with the side chain residue; Arg 52 (3.55 Å) at a strength of 0.6 %. Furthermore, it showed the presence of two arene hydrogen interactions between tetrahydroquinoline moiety and benzochromine moiety with the side chain residues; Arg 52 and Ala 19; respectively, beside many hydrophobic interactions between other atoms of the compound and the following amino acid residues; Ala 7, Ile 14, Gly 15, Met 16, Glu 17, Asn 18, Ala 19, Met 20, Asp 27, Phe 31, Lys 32, Thr 46, Ser 49, Arg 52, Leu 54, Arg 57, Ile 94, Gly 95, Gly 96, Tyr 100 and Thr 123, as shown in **Figure 4**.

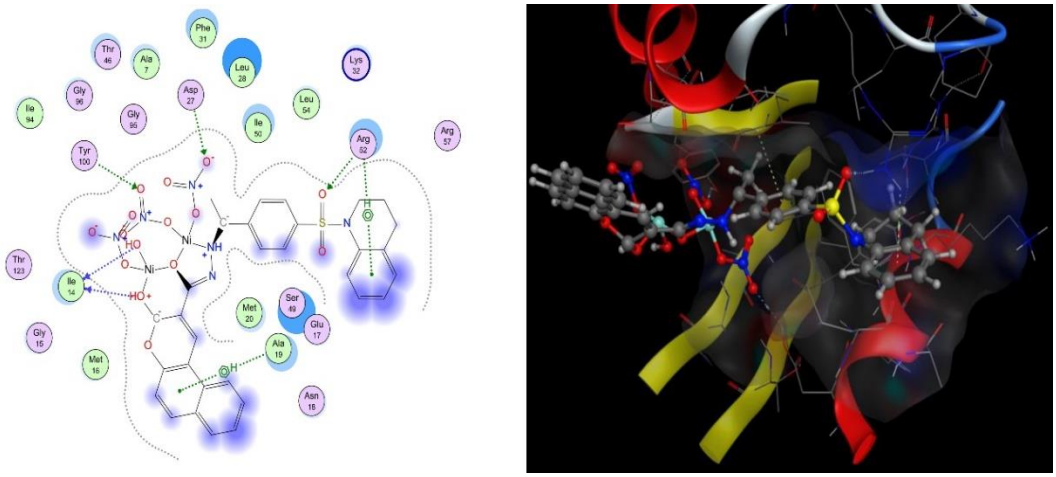

Figure 4: Docking of Complex **2** into DHFR

3.6.5. Docking of compound 3 into DHFR:

Active site showed the interaction of two oxygen atoms of nitroso functions as it acted as a hydrogen bond acceptor with the side chain residues; Trp 22 and Tyr 100 (3.42 Å, 2.82 Å) at a strength of 1.1% and 1.9%; respectively. Moreover, one oxygen atom of sulfonyl moiety acted as a hydrogen bond acceptor with the side chain residue; Arg 52 (2.88 Å) at a strength of 2.4 %. In addition to hydrophobic interactions concerning other atoms of the compound and the following amino acid residues: Ala 7, Ile 14, Gly 15, Met 16, Glu 17, Asn 18, Ala 19, Met 20, Trp 22, Asp 27, Leu 28, Phe 31, Lys 32, His 45, Thr 46, Ser 49, Arg 52, Leu 54, Arg 57, Ile 94, Gly 95, Gly 96, Tyr 100 and Thr 123, as shown in **Figure 5**.

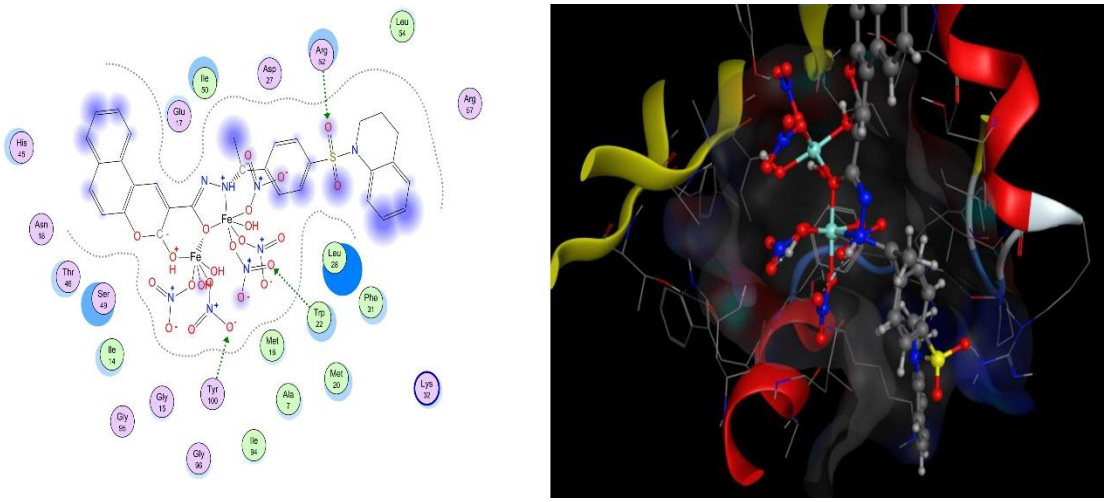

Figure 5: Docking of Complex **3** into DHFR

3.6.6. Docking and molecular modeling (Conclusion)

Docking was made for the compounds **HL**, **1**, **2**, and **3** on the DHFR in a trial to expect their method of act as anticancer drugs. Compound **HL** and **2**, which suggest that they might utilize their action through inhibition of the DHFR enzyme, **Table 5**. It is clear from the present data that the comparison of the docking score energy for the compounds follows the order **HL > 2 > 3 > 1**.

Table 1. Anti-microbial activity of newly synthesized compounds [a]

Comp. No.	Fungi		Bacteria						
			Gram-positive			Gram-negative			
	Aspergillus fumigatus (RCMB 02568)	Candida albicans (RCMB 05036)	Staphylococcus aureus (RCMB 010027	Streptococcus pneumoniae (RCMB 010010)	Bacillis subtillis (RCMB 010067)	Pseudomonas aeruginosa (RCMB 010043-6)	Salmonella Typhimurium (RCMB 010315-4)	Klebsiella pneumoniae (RCMB 010096-5)	Escherichia coli (RCMB 010052-3)
HL	19.6 ± 1.2	16.2 ± 1.5	15.2 ± 0.63	13.6 ± 1.2	15.4 ± 0.63	NA[c]	13.6 ± 1.2	17.3 ± 0.58	12.8 ± 0.63
1	18.1 ± 0.63	16.3 ± 0.63	16.2 ± 1.5	15.4 ± 1.5	16.3 ± 0.63	NA[c]	15.2 ± 1.5	16.2 ± 0.63	13.9 ± 1.5
2	25.3 ± 0.58	22.6 ± 1.2	25.7 ± 0.63	28.3 ± 0.72	30.4 ± 0.63	21.3 ± 1.2	25.3 ± 0.63	26.4 ± 1.5	22.6 ± 1.2
3	22.1 ± 1.2	19.2 ± 1.5	20.6 ± 1.2	24.3 ± 1.2	26.3 ± 0.58	18.4 ± 0.72	20.4 ± 0.63	23.6 ± 1.5	21.4 ± 1.5
St[b].	23.2 ± 0.58	22.1 ± 0.63	25.7 ± 0.63	24.3 ± 0.58	27.2 ± 1.2	22.3 ± 0.63	24.2 ± 1.2	23.4 ± 0.58	25.4 ± 0.63

[a] Mean zone of inhibition in mm ± standard deviation (S.D.).
[b] Standard controls for the microorganisms are "Amphotericin B" for the Fungi, "Ampicillin" for the Gram-positive bacteria and "Ciprofloxacin" for the Gram-negative bacteria.
[c] NA: No activity.

Table 2. Anti-mycobacterium tuberculosis (TB) activity of newly compounds.

Comp. No.	Inhibitory %
HL	0
1	0
2	68.32 ± 1.2
3	71.32 ± 1.5
St[a]	83.2 ± 2.1

[a] The standard control is isoniazid. Each value is the mean of three experiments ± standard error (SD)

Table 3. Cytotoxic activity of all prepared compounds against human liver carcinoma "**HEPG2**" cell line at different concentrations [a]

Comp. No.	Validity for sample Conc. (µg/mL)					µM	
	50	25	12.5	6.25	3.125	IC_{50}	IC_{50}
HL	70.86 ± 3.91	87.12 ± 0.53	94.08 ± 0.24	97.23 ± 0.06	99.64 ± 0.04	98.3	178.21
1	77.82 ± 0.26	84.06 ± 0.19	91.75 ± 0.25	98.02 ± 0.12	100	257	390.30
2	91.48 ± 0.23	98.06 ± 0.14	100	100	100	284	325.68
3	97.13 ± 0.34	99.54 ± 0.12	100	100	100	> 400	389.73
MTX	71.27± 1.71	90.21 ± 0.02	95.71 ± 1.01	98.91 ± 0.31	100	109	239.86

[a] The standard control is methotrexate (MTX). Each value is the mean of three experiments ± standard error (SD)

Table 4. Cytotoxic activity of all prepared compounds against human prostatecarcinoma**"PC3"**cell line at different concentrations [a]

Comp. No.	Validity for sample Conc. (µg/mL)					µM	
	50	25	12.5	6.25	3.125	IC_{50}	IC_{50}
HL	46.72 ± 3.16	81.91 ± 2.89	95.16 ± 0.35	99.24 ± 0.12	100	47.7	86.47
1	11.76 ± 0.12	19.48 ± 0.26	27.64 ± 0.82	35.87 ± 1.91	47.62 ± 1.01	2.89	4.39
2	16.48 ± 0.26	28.63 ± 0.51	40.96 ± 2.42	58.65 ± 3.79	76.21 ± 0.85	9.31	10.68
3	38.26 ± 2.38	54.82 ± 3.79	68.93 ± 1.21	85.25 ± 0.79	92.71 ± 0.57	32.3	31.47
MTX	19.32 ± 1.23	32.91 ± 0.93	45.28 ± 2.10	63.79 ± 2.94	80.38 ± 0.21	13.7	30.15

[a] The standard control is methotrexate (MTX). Each value is the mean of three experiments ± standard error (SD)

Table 5: Docking score energy of the newly synthesized compounds

Comp. No.	Score	E_conf	E_place	E_score1	E_refine	E_score2
HL	-24.0578	146.5361	-101.974	-11.5337	46.65773	-24.0578
1	-6.87546	135.912	-88.1974	-10.5648	-19.7365	-6.87546
2	-8.19287	-660.481	-92.7861	-9.76687	-19.8851	-8.19287
3	-7.33954	-1331.69	-121.332	0.00	-9.14158	-7.33954

Score; for all scoring functions, lower scores indicate more favorable poses. The unit for all scoring functions is kcal / mol. The London dG scoring function estimates the free energy of binding of the ligand from a given pose. **E_conf;** the energy of the conformer. If there is a refinement stage, this is the energy calculated at the end of the refinement. **E_place;** Score from the placement stage (*Placement*. A collection of poses is generated from the pool of ligand conformations using one of the placement methods).**E_score1;** Score from the 1strescoring stage. **E_refine;** Score from the refinement stage (Refinement. Energy minimization of the system is carried out using the conventional molecular mechanics setup).**E_score2;** Score from the 2nd rescoring stage.

Table 6: Physical and analytical data of all newly synthesized compounds

Comp. No.	Molecular formula	M. Wt.	Yield %	Color	M.P. (^{o}C)	Calc. (Found)%				
						C	H	N	S	M
HL	$C_{31}H_{25}N_3O_5S$	551.61	87.3	Yellow	270-271	67.50 (67.33)	4.57 (4.27)	7.62 (7.47)	5.81 (5.59)	---
1	$C_{31}H_{24}AgN_3O_5S$	658.47	76.5	Pale brown	244-245	56.54 (56.33)	3.67 (3.49)	6.38 (6.10)	4.87 (4.60)	16.38 (16.14)
2	$C_{31}H_{26}N_6Ni_2O_{15}S$	872.02	65.4	Yellow	250-252	42.70 (42.64)	3.01 (2.89)	9.64 (9.40)	3.68 (3.38)	13.46 (13.22)
3	$C_{31}H_{30}Fe_2N_8O_{23}S$	1026.4	63.9	Brown	300-301	36.28 (36.07)	2.95 (2.71)	10.92 (10.73)	3.12 (3.00)	10.88 (10.72)

4. CONCLUSION

Three novel complexes with Schiff bases derived from 2-cyano-*N'*-(1-(4-((3,4-dihydroquinolin-1(2*H*)-yl)sulfonyl)phenyl)ethylidene)aceto-hydrazide and 2-hydroxy-1-naphthaldehyde were prepared and characterized *via* physicochemical and spectroscopic method. All the newly synthesized compounds were tested *in-vitro* anti-microbial. Ni(II) complex showed a significant activity against all microorganisms. Fe(III) complex exhibits a significant activity against Mycobacterium tuberculosis. The *in vitro* anti-cancer activity showed that the ligand exhibited a significant inhibition against human liver carcinoma HEPG2 cell line with IC_{50} value 178.21 µM. while, Ag(I) and Ni(II) complexes exhibited a significant inhibition against human prostate carcinoma PC3 cell line with IC_{50} values 4.39 µM., and 10.68 µM., respectively compared to MTX as a reference drug.

REFERENCES

1. S. A. Abbas, M. Munir, A. Fatima, S. Naheed, Ilyas, Z. *Electronic J. Life Sci.* **2010**, *1*, 37-40.
2. P. S. Salve, S. G. Alegaon, D. Sriram. Bioorg. Med. Chem. Lett. **2017**, 27(8), 1859-1866.
3. T. S. Basu Baul, P. Kehie, A. Duthie, N. Guchhait, N. Raviprakash, R. B. Mokhamatam, S. K. Manna, N. Armata, M. Scopelliti, R. Wang, U. Englert. J. Inorg. Biochem. **2017**, *168*, 76-89.
4. E. L. Araujo, H. F. G. Barbosa, E. R. Dockal, E. T. G. Cavalheiro. Inter. J. Bio. Macro. **2017**, *95*, 168-176.
5. M.A. Bhat, M.Imran, S. A.Khan, N. Siddiqui, *J. Pharm. Sci.* **2005**, *67*, 151-159.
6. L. Wang, Y. Feng, J. Xue, Y. Li, *J. Serbian Chem. Soc.* **2008**, *73*, 1-6.
7. S.J. Wadher, M. P. Puranik, N. A. Karande, P. G. Yeole, Inter. *J. Pharm. Tech. Res.* **2009**, *1*, 22-33.
8. J.S. Hadi, B. K. Alsalami, A. H. Essa, *J. Scientific Res.* **2009**, *3*, 563-568.
9. G. Melagraki, A. Afantitis, H.Sarimveies, O. L. Markopoulou, C. T. Supuran, *Bioorg. Med. Chem.* **2006**, *14*, 1108-1114.
10. Z.H. Chohan, H. Pervez, A. Rauf, K. M. Khalid, C. T. Supuran, *J. Enz. Inh. Med. Chem.* **2006**, *21*, 193-201.
11. J.Joseph, K.Nagashri, J. G. Boomadevi, *Eur. J. Med. Chem.* **2012**, *49*, 151-163.
12. Y. L. Chen, K. C. Fang, J. Y. Sheu, S. L. Hsu, C. C. Tzeng, *J. Med. Chem.* **2001**, *44*, 2374-2377.
13. M. G. Banwell, *Pure Appl. Chem.* **2008**, *80*, 669-679.
14. E. Abele, R. Abele, E. Lukevics,*Chem. Heterocycl. Comp.* **2008**, *44*, 769-792.
15. Barluenga, J.; Rodriguez, F.; Fananas, F. *J. Chem. Asian J.* **2009**, *4*, 1036-1048.
16. S. Kumar, S. Bawa, H. Gupta, *Mini Rev. Med. Chem.* **2009**, *9*, 1648-1654.
17. S. Bawa, S. Kumar, S. Drabu, R. *J.* Kumar, *Pharm. Bioallied Sci.* **2010**, *2*, 64-71.
18. N. Qizilbash, A. Whitehead, J. Higgins, G. Wilcock, L.Schneider, M. *J.* Farlow, *Am. Med. Assoc.* **1998**, *280*, 1777-1782.

19. R. W. Clark, R. B. Ruggeri, D.Cunningham, M. J. Bamberger, *J. Lipid. Res.* **2006**, *47*, 537-552.

20. X. Jia, Han, B. W Zhang, X.Jin, L.Yang, Z.L. Liu, *Synthesis*, **2006**, *17*, 2831-2836.

21. M.G.Papich, J.E. Riviere, Fluoroquinolone antibacterial drugs: Veterinary Pharmacology and Therapeutics, 9th Edition, Wiley-Blackwell, Iowa State University Press, USA, **2009**, pp. 983-1011.

22. P.Jain, C. Saravanan, S.K. Singh, *Eur. J. Med. Chem.* **2013**, *60*, 89-100.

23. G.Melagraki, A. Afantitis, H. Sarimveis, O. Igglessi-Markopoulou, C.T. Supuran, Bioorg. *Med. Chem.* **2006**, *14(4),* 1108-1114.

24. N.Anand, M.E. Wolff, Burger's medicinal chemistry and drug discovery. In Therapeutic Agents, 5th Edition, J. Wiley & Sons, New York, **1996** pp. 527-544.

25. P.Ortqvist, S. D. Peterson, E.Kerblom, T.Gossas, Y. A. Sabnis, R. Fransson,G. Lindeberg, H. U. Danielson, A Karlen, A. Sandstrom, *Bioorg. Med. Chem.* **2007**, *15*, 1448-1453.

26. D.Mandloi, S. Joshi, P.V. Khadikar, N. Khosla, *Bioorg. Med. Chem. Lett.* **2005**, *15(2),* 405-411.

27. D.Vullo, B. Steffansen, B. Brodin, C.T. Supuran, A. Scozzafava,C.U. Nielsen, *Bioorg. Med. Chem.* **2006**, *14(7)*, 2418-2427.

28. S.A.Al- Harbi, M.S. Bashandy,H.M. Al- Saidi, A.A.A. Emara, T.A.A. Mousa, *Spectrochim. Acta A*. **2015**, *145*, 425- 439.

29. R.J.Hay, M.M. Cleland, S. Durkin, Y.A.Reid, Cell Line Preservation and Authentication in "Animal Cell Culture", (Ed. J. R. W. Masters), Oxford University Press, New York, **2000**.

30. A. P. Wilson, Cytotoxicity and Viability Assays in Animal Cell Culture: A Practical Approach, 3rd edition, (Ed. J. R. W. Masters), Oxford University Press, New York, **2000**.

31. Y. Saintigny, K.Makienko, C.Swanson, M. J. Emond, J. R. Monnat, *Mol. Cell Biol.* **2004**, *2*, 6971- 6978.

32. D.Cheng, J.Yang, Y.Zhao, *Chinese Med. Equip. J.* **2004**, *4*, 26-32.

33. R. R. Hafidh, A.Abdulamir, F.Abu Bakar, F. A. Jalilian, F.Abas, Z.Sekawi, *BMC Compl. Altern. Med.* **2012**, *12(1),* 208- 218.

34. J. D. Chellaian, J.Johnson, *Spectrochim. Acta A.* **2014**, *127*, 396- 404.

35. A.Suga, T.Narita, L.Zhou, Sakagami, H.; Satoh, K.; Wakabayashi, H. *In Vivo* **2009**, *23*, 691- 698.

36. Q. R.Du, D. D. Li, Y. Z. Pi, J. R. Li, J. Sun, F. Fang, W. Q. Zhong, H. B. Gong, H.L.Zhu, *Bioorg. Med. Chem.* **2013**, *21*, 2286- 2297.

37. K. N. Rao, S. R. Venkatachalam, *Bioorg. Med. Chem.* **1999**, *7*, 1105-1110.

38. S.Vilar, G.Cozza; S. Moro, *Curr. Top. Med. Chem.* **2008**, *8(18),* 1555-1572.

39. A. M. Nassar, A. M. Hassan, S. S. Alabd, Syn. Rea. Inorg. Metal-Org. Nano-Metal Chem. **2015**, *45(2),* 256-270.

40. G.Socrates, Infrared and Raman characteristic group frequencies: tables and charts. John Wiley & Sons, **2004**.

41. H. A. Chu, H. Sackett, G. T. Babcock, Biochemistry **2000**, *39(47)*, 14371-14376.

42. S.Gourbatsis, N.Hadjiliadis, S. P. Perlepes, A.Garoufis, I. S. Butler, Transition Metal Chem. **1998**, *23(5)*, 599-604.

43. A. M. Hassan, A. M. Nassar, Y. Z. Hussien, A. N. Elkmash, Applied biochem. Biotech. **2012**, *167(3)*, 581-594.

44. S. Chandra, K. Gupta, Transition Metal Chem. **2002**, *27(2)*, 196-199.

45. A. P. B Lever, Inorganic Electronic Spectroscopy, 2nd edition Elsevier, New York, NY, USA, **1984**.

Corresponding author: Mahmoud Sayed Bashandy,

Department of Chemistry, University College in Al- Jamoum, Umm Al- Qura University, 21955, Makkah, Saudi Arabia.

On line publication Date: 07.06.2017